Journal of Magnetic Resonance 198 (2009) 174–182

Contents lists available at ScienceDirect

Journal of Magnetic Resonance

journal homepage: www.elsevier.com/locate/jmr

Extension of the double-wave-vector diffusion-weighting experiment to multiple concatenations

Jürgen Finsterbusch *

Department of Systems Neuroscience, University Medical Center Hamburg–Eppendorf, Hamburg, Germany
Neuroimage Nord, University Medical Centers Hamburg–Kiel–Lübeck, Hamburg–Kiel–Lübeck, Germany

ARTICLE INFO

Article history:
Received 12 December 2008
Revised 6 February 2009
Available online 13 February 2009

Keywords:
Double-wave-vector diffusion-weighting
Multiple-wave-vector diffusion-weighting
Restricted diffusion
Cell size
Pore size

ABSTRACT

Experiments involving two diffusion-weightings in a single acquisition, so-called double- or two-wave-vector experiments, have recently been applied to measure the microscopic anisotropy in macroscopically isotropic samples or to estimate pore or compartment sizes. These informations are derived from the signal modulation observed when varying the wave vectors' orientations. However, the modulation amplitude can be small and, for short mixing times between the two diffusion-weightings, decays with increased gradient pulse lengths which hampers its detectability on whole-body MR systems. Here, an approach is investigated that involves multiple concatenations of the two diffusion-weightings in a single experiment. The theoretical framework for double-wave-vector experiments of fully restricted diffusion is adapted and the corresponding tensor approach recently presented for short mixing times extended and compared to numerical simulations. It is shown that for short mixing times (i) the extended tensor approach well describes the signal behavior observed for multiple concatenations and (ii) the relative amplitude of the signal modulation increases with the number of concatenations. Thus, the presented extension of the double-wave-vector experiment may help to improve the detectability of the signal modulations observed for short mixing times, in particular on whole-body MR systems with their limited gradient amplitudes.

1. Introduction

Experiments where two diffusion-weighting periods are applied successively in a single acquisition [1–4] (Fig. 1a) have gained interest due to their sensitivity to tissue structure on a microscopic level. Because of the analogy of a diffusion-weighting period to a scatter event for short gradient pulses [5], these experiment often are referred to as two- or double-wave-vector (DWV) experiments, in contrast to standard, single-wave-vector diffusion-weighting. In these experiments, the dependency of the signal amplitudes on the angle between the two wave vectors is usually exploited since it offers information beyond that of a single-wave-vector experiment. Because the averaging over the sample is performed for the accumulated phase difference each spin experiences during the two successive diffusion-weightings with, in general, different directions, the correlation of the diffusion-related displacements are reflected in the acquired signal. This information can be used to assess the size and shape of the compartments in which the spins diffuse [3].

Which property can be investigated depends on the experimental parameters, in particular on the mixing time between the two diffusion-weightings. For long mixing times and diffusion in isotropically orientation-distributed pores or cells, an angular modulation occurs only for anisotropic, e.g. ellipsoidal, cells yielding a signal difference between parallel and perpendicular orientations of the wave vectors [3]. This is in particular interesting as such a sample in a standard, single-wave-vector experiment appears isotropic and cannot be distinguished from a sample of spherical pores. Experiments showing this effect have been reported for yeast cells [6], model systems [7], and, *ex vivo*, for monkey brain gray matter [7] and pig spinal cord [8]. The observations have been supported by theoretical considerations [6] and numerical simulations [9,10].

For short mixing times, a signal difference between parallel and antiparallel wave vector orientations is expected [3] which has been demonstrated for biological model systems and pig spinal cord *ex vivo* on a whole-body MR system [11]. Furthermore, experimental evidence of this signal difference in the cortico-spinal tract in the living human brain has been provided recently [12]. Because the initial description of this effect [3] assumed infinitely short gradient pulses and mixing times, infinitely long diffusion times, and was focused on isotropically orientation-distributed pores or cells, some theoretical extensions have been provided which cover

* Address: Institut für Systemische Neurowissenschaften, Geb. W34, Universitätsklinikum Hamburg–Eppendorf, 20246 Hamburg, Germany. Fax: +49 40 7410 59955.
E-mail address: j.finsterbusch@uke.uni-hamburg.de

1090-7807/$ - see front matter © 2009 Elsevier Inc. All rights reserved.
doi:10.1016/j.jmr.2009.02.003

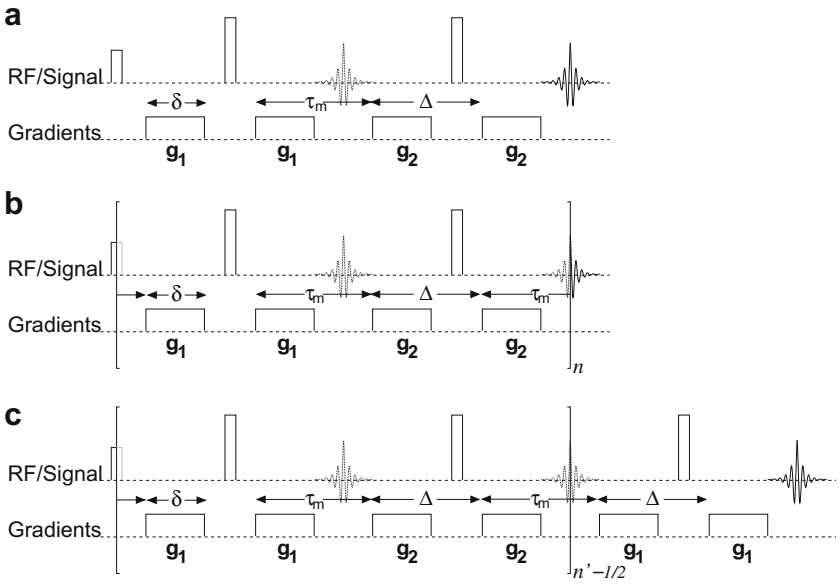

Fig. 1. Basic pulse sequences for the double-wave-vector (DWV) diffusion-weighting experiments considered. (a) Standard DWV experiment, (b) extension with n concatenations of the two wave vectors which involves an even number of diffusion-weightings, and (c) extension with concatenations of the two wave vectors and a final diffusion-weighting with the first wave vector, i.e. an odd number of diffusion-weightings, which can be considered as an experiment with a half-integral number n' of concatenations.

signal expressions for finite timing parameters [13] and a tensor approach to describe the signal behavior for arbitrary orientation-distributions and obtain a rotationally-invariant pore size measure [14].

The amplitude of the signal differences observed in the mentioned experiments is rather small and limits their detectability. This in particular holds for whole-body MR systems with their weaker gradient systems and the experiment with short mixing time to determine cell or compartment sizes where the signal modulation has been shown to decay with the gradient pulse length [9,10,15,16].

In this work, an extension of the DWV experiment is investigated which involves multiple concatenations of the two diffusion-weightings. The theoretical framework derived for fully restricted diffusion is adapted yielding expressions for the signal in such experiments. The corresponding tensor approach for short mixing times and the derived pore or cell size measure [14] are extended and verified by numerical simulations. It is shown theoretically and in numerical simulations that the relative amplitude of the signal modulation for short mixing times increases with the number of concatenations which may help to improve the detectability of the signal modulation experimentally and to increase the accuracy of the derived cell parameters.

2. Theory

A first analysis of the MR signal in experiments involving multiple wave vector diffusion-weighting (e.g. see Fig. 1a) was presented by Mitra [3]. In the short-pulse approximation, i.e. assuming that the gradient pulse duration δ approaches 0, the phase difference $\Delta\varphi$ for a particle diffusing along the trajectory $\mathbf{r}(t)$ in the experiment shown in Fig. 1a is given by

$$\Delta\varphi(\mathbf{q_1},\mathbf{q_2}) = \mathbf{q_1}[\mathbf{r}(0)-\mathbf{r}(\Delta)] + \mathbf{q_2}[\mathbf{r}(2\Delta+\tau_m)-\mathbf{r}(\Delta+\tau_m)] \quad (1)$$

where $\mathbf{q_1}$ and $\mathbf{q_2}$ represent the two wave vectors and are given by $\mathbf{q_i} = \gamma\delta g_i$ with the gyromagnetic ratio γ and the gradient pulse duration and amplitude δ and g_i, respectively. The corresponding MR signal then obeys

$$M(\mathbf{q_1},\mathbf{q_2}) \propto \langle e^{i\mathbf{q_1}[\mathbf{r}(0)-\mathbf{r}(\Delta)]+i\mathbf{q_2}[\mathbf{r}(2\Delta+\tau_m)-\mathbf{r}(\Delta+\tau_m)]}\rangle \quad (2)$$

where the average is taken over the spin ensemble within the sample.

Considering spins diffusing in isolated pores, i.e. fully restricted diffusion, and assuming furthermore that the diffusion time Δ is large compared to $\tau_D = \frac{a^2}{2D}$ ($\Delta \gg \tau_D$), i.e. the time a spin with diffusion coefficient D typically requires to cross a pore with diameter a, some simplifications of Eq. (2) can be achieved. Thereby, two limiting cases for the mixing time τ_m between the two diffusion-weightings, a vanishing and a very large τ_m, were considered in more detail [3].

For a long mixing time ($\tau_m \gg \tau_D$), the individual $\mathbf{r}$ for a spin's trajectory at the individual time points in Eq. (2) are independent and their ensemble averages are identical. This yields

$$M(\mathbf{q_1},\mathbf{q_2}) \propto \sum_i |\tilde{\rho}_i(\mathbf{q_1})|^2 |\tilde{\rho}_i(\mathbf{q_2})|^2 \quad (3)$$

with

$$\tilde{\rho}_i(\mathbf{q}) = \int_{\text{pore}} \rho_i(\mathbf{r}) e^{i\mathbf{q}\mathbf{r}} d\mathbf{r} \quad (4)$$

being the Fourier transform of the spin density $\rho_i(\mathbf{r})$ in the ith pore.

For a very short mixing time ($\tau_m \to 0$), the positions at Δ and $\Delta+\tau_m$ are identical while those at 0, Δ, and 2Δ are independent and yield the same ensemble average. Thus, an MR signal of

$$M(\mathbf{q_1},\mathbf{q_2}) \propto \sum_i \tilde{\rho}_i(\mathbf{q_1})\tilde{\rho}_i(\mathbf{q_2})\tilde{\rho}_i(-\mathbf{q_1}-\mathbf{q_2}) \quad (5)$$

is obtained.

2.1. Signal for multiple concatenations of two wave vectors

Now the experiment sketched in Fig. 1b is investigated which involves a concatenation of diffusion-weightings where the wave vector alternates between $\mathbf{q_1}$ and $\mathbf{q_2}$. This experiment represents a special case of the general multiple-wave-vector experiment

where all odd and all even wave vectors are identical ($\mathbf{q_{2j+1}} = \mathbf{q_1}$, $\mathbf{q_{2j}} = \mathbf{q_2}$). Furthermore, all diffusion times as well as all mixing times are assumed to be identical ($\Delta_j = \Delta$, $\tau_{mj} = \tau_m$), respectively. Thus, the extra degrees of freedom an experiment with more than two wave vectors offers are not exploited. This is why the term "double wave vector" will still be used to describe the experiment.

Unless stated otherwise, it is assumed that both wave vectors are used n times, i.e. $n_1 = n_2 = n$ where the n_i indicate how often wave vector i is applied. Thus, the equation derived in the following section must match the results presented in the previous section if n is set to 1.

The phase difference an individual spin accumulates in the jth concatenation can be obtained by replacing each $\mathbf{r}(t)$ in Eq. (1) by $\mathbf{r}(t + 2j(\Delta + \tau_m))$ because $2(\Delta + \tau_m)$ is the duration of one concatenation ($j = 0 \ldots n-1$). Thus, the total phase difference is given by

$$\begin{aligned}\Delta\varphi(\mathbf{q_1},\mathbf{q_2}) = \sum_{j=0}^{n-1} \{&\mathbf{q_1}[\mathbf{r}(2j(\Delta+\tau_m)) - \mathbf{r}(2j(\Delta+\tau_m)+\Delta)] \\ &+ \mathbf{q_2}[(\mathbf{r}((2j+1)(\Delta+\tau_m)+\Delta) - \mathbf{r}((2j+1)(\Delta+\tau_m))]\}\end{aligned} \tag{6}$$

and the MR signal of the sample obeys

$$M(\mathbf{q_1},\mathbf{q_2}) \propto \left\langle \prod_{j=0}^{n-1} e^{i\mathbf{q_1}[\mathbf{r}(2j(\Delta+\tau_m)) - \mathbf{r}(2j(\Delta+\tau_m)+\Delta)] + i\mathbf{q_2}[\mathbf{r}((2j+1)(\Delta+\tau_m)+\Delta) - \mathbf{r}((2j+1)(\Delta+\tau_m))]} \right\rangle. \tag{7}$$

For the case of a long mixing time ($\tau_m \gg \tau_D$), the arguments provided in the previous section apply analogously, i.e. the values of the trajectory $\mathbf{r}$ at all time points occurring in Eq. (7), i.e. $2j(\Delta + \tau_m)$, $2j(\Delta + \tau_m) + \Delta$, $(2j+1)(\Delta + \tau_m) + \Delta$, and $(2j+1)(\Delta + \tau_m)$, are independent for any j which yields an MR signal of the sample of

$$M(\mathbf{q_1},\mathbf{q_2}) \propto \sum_i |\tilde{\rho}_i(\mathbf{q_1})|^{2n} |\tilde{\rho}_i(\mathbf{q_2})|^{2n}. \tag{8}$$

For a vanishing mixing time ($\tau_m = 0$), the time points $2j(\Delta + \tau_m) + \Delta$ and $(2j+1)(\Delta + \tau_m)$ coincide for $0 \leqslant j \leqslant n-1$ at the transition from $\mathbf{q_1}$ to $\mathbf{q_2}$ (inner-cycle transition). But also $(2j+1)(\Delta + \tau_m) + \Delta$ and $2j'(\Delta + \tau_m)$ are identical for $j' = j + 1$ and $0 \leqslant j < n-1$ reflecting the transition from $\mathbf{q_2}$ of one concatenation to the $\mathbf{q_1}$ of the next concatenation (inter-cycle transition). This yields a MR signal of

$$M(\mathbf{q_1},\mathbf{q_2}) \propto \sum_i \tilde{\rho}_i(\mathbf{q_1})\tilde{\rho}_i(\mathbf{q_2})\tilde{\rho}_i(-\mathbf{q_1}-\mathbf{q_2})^n \tilde{\rho}_i(\mathbf{q_1}+\mathbf{q_2})^{n-1} \tag{9}$$

where $\tilde{\rho}_i(-\mathbf{q_1} - \mathbf{q_2})^n$ represents the n inner-cycle transitions and $\tilde{\rho}_i(\mathbf{q_1} + \mathbf{q_2})^{n-1}$ the $n-1$ inter-cycle transitions, respectively. Because ρ is real, $\tilde{\rho}_i(\mathbf{q_1} + \mathbf{q_2}) = \tilde{\rho}_i^*(-\mathbf{q_1} - \mathbf{q_2})$ which implies that the MR signal can be written as

$$M(\mathbf{q_1},\mathbf{q_2}) \propto \sum_i \tilde{\rho}_i(\mathbf{q_1})\tilde{\rho}_i(\mathbf{q_2})\tilde{\rho}_i(-\mathbf{q_1}-\mathbf{q_2})^n \tilde{\rho}_i^*(-\mathbf{q_1}-\mathbf{q_2})^{n-1} \tag{10}$$

where $\tilde{\rho}_i(-\mathbf{q_1} - \mathbf{q_2})$ and $\tilde{\rho}_i^*(-\mathbf{q_1} - \mathbf{q_2})$ were used to emphasize the analogy to Eq. (5).

2.2. Adaptation of tensor approach and pore size measure for a vanishing mixing time

For the concatenated experiment, the recently presented tensor approach [14] which can be used to describe the general signal behavior for a vanishing mixing time, needs to be adapted. The derivation of the extended model is sketched in the following paragraphs, more details can be found in [14].

Considering a single pore orientation, the pore index i can be ignored and Eq. (10) simplifies to

$$M(\mathbf{q_1},\mathbf{q_2}) \propto \tilde{\rho}(\mathbf{q_1})\tilde{\rho}(\mathbf{q_2})\tilde{\rho}(-\mathbf{q_1}-\mathbf{q_2})^n \tilde{\rho}^*(-\mathbf{q_1}-\mathbf{q_2})^{n-1} \tag{11}$$

Introducing the six-element vector $\mathbf{Q} = (q_1^T, q_2^T)^T$, i.e.

$$Q_i = \begin{cases} (\mathbf{q_1})_i & \text{for } i = 1,2,3 \\ (\mathbf{q_2})_{i-3} & \text{for } i = 4,5,6 \end{cases}, \tag{12}$$

Eq. (10) can be re-written as

$$M(\mathbf{Q}) \propto \tilde{\rho}_1(\mathbf{Q})\tilde{\rho}_2(\mathbf{Q})\tilde{\rho}_3(\mathbf{Q}) \tag{13}$$

with

$$\begin{aligned}\tilde{\rho}_1(\mathbf{Q}) &= \tilde{\rho}(Q_1,Q_2,Q_3) = \tilde{\rho}(\mathbf{q_1}) \\ \tilde{\rho}_2(\mathbf{Q}) &= \tilde{\rho}(Q_4,Q_5,Q_6) = \tilde{\rho}(\mathbf{q_2}) \\ \tilde{\rho}_3(\mathbf{Q}) &= \tilde{\rho}(-Q_1-Q_4,-Q_2-Q_5,-Q_3-Q_6)^n \\ &\quad \tilde{\rho}^*(-Q_1-Q_4,-Q_2-Q_5,-Q_3-Q_6)^{n-1} \\ &= \tilde{\rho}(-\mathbf{q_1}-\mathbf{q_2})^n \tilde{\rho}^*(-\mathbf{q_1}-\mathbf{q_2})^{n-1}.\end{aligned} \tag{14}$$

Compared to the previous definitions for a single concatenation [14], only $\tilde{\rho}_3$ has to be generalized while the other two terms are independent of the number of concatenations.

To expand $M(\mathbf{Q})$ to second order, the Taylor expansions of $\tilde{\rho}$ and $\tilde{\rho}^*$ are required which are identical and given by

$$\tilde{\rho}(\mathbf{q}) = V - \frac{1}{2}\mathbf{q}^T \underline{\underline{\mathbf{R}}}\, \mathbf{q} + \mathcal{O}(q^3) \;= \tilde{\rho}^*(\mathbf{q}) \tag{15}$$

with the pore volume V and the 3×3 tensor $\underline{\underline{\mathbf{R}}}$ whose elements are

$$R_{ij} = \int_{\text{pore}} \rho(\mathbf{r}) r_i r_j \, d\mathbf{r}. \tag{16}$$

This yields

$$\tilde{\rho}_1(\mathbf{Q}) = V - \frac{1}{2}\mathbf{Q}^T \begin{pmatrix} \underline{\underline{\mathbf{R}}} & 0 \\ 0 & 0 \end{pmatrix} \mathbf{Q} + \mathcal{O}(Q^3). \tag{17}$$

and

$$\tilde{\rho}_2(\mathbf{Q}) = V - \frac{1}{2}\mathbf{Q}^T \begin{pmatrix} 0 & 0 \\ 0 & \underline{\underline{\mathbf{R}}} \end{pmatrix} \mathbf{Q} + \mathcal{O}(Q^3). \tag{18}$$

For $\tilde{\rho}_3$, the corresponding expansions of $\tilde{\rho}^{(*)}(\mathbf{q})^m$ are needed and can be calculated to

$$\tilde{\rho}^{(*)}(\mathbf{q})^m = V^m - \frac{1}{2} m V^{m-1} \mathbf{q}^T \underline{\underline{\mathbf{R}}}\, \mathbf{q} + \mathcal{O}(q^3) \tag{19}$$

where again was used that

$$\frac{\partial}{\partial q_k}\tilde{\rho}(\mathbf{q})\bigg|_{q_k=0} = 0 \tag{20}$$

vanishes if the center of mass is chosen as the point of origin. Thus,

$$\tilde{\rho}(\mathbf{q})^n \tilde{\rho}^*(\mathbf{q})^{n-1} = V^{2n-1} - \frac{1}{2}(2n-1)V^{2n-2}\mathbf{q}^T \underline{\underline{\mathbf{R}}}\, \mathbf{q} + \mathcal{O}(q^3) \tag{21}$$

and

$$\tilde{\rho}_3(\mathbf{Q}) = V - \frac{1}{2}(2n-1)\mathbf{Q}^T \begin{pmatrix} \underline{\underline{\mathbf{R}}} & \underline{\underline{\mathbf{R}}} \\ \underline{\underline{\mathbf{R}}} & \underline{\underline{\mathbf{R}}} \end{pmatrix} \mathbf{Q} + \mathcal{O}(Q^3). \tag{22}$$

This yields the same tensor equation as in [14]

$$M_n(\mathbf{Q}) \propto V - \frac{1}{2}\mathbf{Q}^T \underline{\underline{\mathbf{T}_n}} \mathbf{Q} \tag{23}$$

but with the modified tensor definition

$$\underline{\underline{\mathbf{T}_n}} = \begin{pmatrix} 2n\underline{\underline{\mathbf{R}}} & (2n-1)\underline{\underline{\mathbf{R}}} \\ (2n-1)\underline{\underline{\mathbf{R}}} & 2n\underline{\underline{\mathbf{R}}} \end{pmatrix}. \tag{24}$$

The adaptation of the pore size measure derived from the trace of the tensor then is straightforward:

$$R_{\mathrm{eff}}^2 = \rho \sum_i \int_{\mathrm{pore}_i} r^2 \, d\mathbf{r} = \mathrm{Tr}(\underline{\underline{\mathbf{R}}}) = \frac{1}{4n}\mathrm{Tr}(\underline{\underline{\mathbf{T}}}_n). \tag{25}$$

This also holds for the reduced tensor formalism [14] which takes only parallel and antiparallel wave vector orientations into account and yields

$$\begin{aligned}\Delta M(\mathbf{q}) &= \frac{1}{2}(2n-1)\left(\mathbf{q}^T\underline{\underline{\mathbf{R}}}\mathbf{q} + \mathbf{q}^T\underline{\underline{\mathbf{R}}}\mathbf{q} - \mathbf{q}^T\underline{\underline{\mathbf{R}}}(-\mathbf{q}) - (-\mathbf{q})^T\underline{\underline{\mathbf{R}}}\mathbf{q}\right) \\ &= \mathbf{q}^T 2(2n-1)\underline{\underline{\mathbf{R}}}\mathbf{q}.\end{aligned} \tag{26}$$

Following the derivation in [14] the signal modulation for a sample with an isotropic orientation-distribution of the pores and for $|\mathbf{q_1}| = |\mathbf{q_2}| = q$ can be calculated to

$$M_{\mathrm{iso}}(q,\theta) \propto V - \frac{1}{3}\rho q^2 \langle R^2\rangle (2n + (2n-1)\cos\theta) \tag{27}$$

where θ is the angle between the two wave vectors and

$$\langle R^2\rangle = \int_{\mathrm{pore}} r^2 \mathrm{d}\mathbf{r} \tag{28}$$

the squared mean radius of gyration of the pore.

2.3. Half-integral number of concatenations

So far, $n_1 = n_2 = n$ was assumed, i.e. the same number of diffusion-weightings for both wave vectors. This yields an experiment that starts with $\mathbf{q_1}$ and terminates with $\mathbf{q_2}$. In principle, one could also use an experiment that terminates with a $\mathbf{q_1}$ without adding the corresponding $\mathbf{q_2}$ required to obtain another full concatenation (Fig. 1c), i.e. where $n_1 = n_2 + 1$. It can be considered as an experiment with an half-integral number of concatenations by defining $n' = (n_1 + n_2)/2 = n_1 - 1/2 = n_2 + 1/2$ as the number of concatenations. In this case, some of the equations presented so far need to be slightly modified and the adapted functions will be denoted by a prime ($'$) in the following paragraphs.

The phase difference then is given by

$$\begin{aligned}\Delta\varphi'(\mathbf{q_1},\mathbf{q_2}) = \sum_{j=0}^{n_2-1} \{&\mathbf{q_1}[\mathbf{r}(2j(\Delta+\tau_m)) - \mathbf{r}(2j(\Delta+\tau_m)+\Delta)] \\ &+\mathbf{q_2}[\mathbf{r}((2j+1)(\Delta+\tau_m)+\Delta) - \mathbf{r}((2j+1)(\Delta+\tau_m))]\} \\ &+\mathbf{q_1}[\mathbf{r}(2n_2(\Delta+\tau_m)) - \mathbf{r}(2n_2(\Delta+\tau_m)+\Delta)]\end{aligned} \tag{29}$$

which yields an MR signal of

$$\begin{aligned}M'(\mathbf{q_1},\mathbf{q_2}) \propto \Bigg\langle \Bigg[\prod_{j=0}^{n_2-1} &e^{i\mathbf{q_1}[\mathbf{r}(2j(\Delta+\tau_m)) - \mathbf{r}(2j(\Delta+\tau_m)+\Delta)] + i\mathbf{q_2}[\mathbf{r}((2j+1)(\Delta+\tau_m)+\Delta) - \mathbf{r}((2j+1)(\Delta+\tau_m))]}\Bigg] \\ &\cdot e^{i\mathbf{q_1}[\mathbf{r}(2n_2(\Delta+\tau_m)) - \mathbf{r}(2n_2(\Delta+\tau_m)+\Delta)]}\Bigg\rangle.\end{aligned} \tag{30}$$

For a long mixing time τ_m,

$$M'(\mathbf{q_1},\mathbf{q_2}) \propto \sum_i |\tilde{\rho}_i(\mathbf{q_1})|^{2n_1} |\tilde{\rho}_i(\mathbf{q_2})|^{2n_2} \tag{31}$$

is obtained. It should be noted that this result is valid for any n_1 and n_2 due to the decoupling of the diffusion-weightings by the long τ_m, i.e. it also holds for $n_1 \neq n_2 + 1$ and any order of the wave vectors.

For the case of a vanishing mixing time ($\tau_m = 0$), the general signal expression then is given by

$$M'(\mathbf{q_1},\mathbf{q_2}) \propto \sum_i \tilde{\rho}_i(\mathbf{q_1})^2 \tilde{\rho}_i(-\mathbf{q_1}-\mathbf{q_2})^{n_1} \tilde{\rho}_i(\mathbf{q_1}+\mathbf{q_2})^{n_2} \tag{32}$$

which simply takes into account that the final, "unpaired" time point now also is related to the first wave vector. Correspondingly,

$$\tilde{\rho}'_1(\mathbf{Q}) = V - \frac{1}{2}\mathbf{Q}^T \begin{pmatrix} 2\underline{\underline{\mathbf{R}}} & 0 \\ 0 & 0 \end{pmatrix} \mathbf{Q} + \mathcal{O}(Q^3) \tag{33}$$

and

$$\tilde{\rho}'_2(\mathbf{Q}) = \underline{\underline{\mathbf{1}}} \tag{34}$$

which yields a tensor of

$$\underline{\underline{\mathbf{T}}}_{n'} = \begin{pmatrix} (2n'+1)\underline{\underline{\mathbf{R}}} & (2n'-1)\underline{\underline{\mathbf{R}}} \\ (2n'-1)\underline{\underline{\mathbf{R}}} & (2n'-1)\underline{\underline{\mathbf{R}}} \end{pmatrix}. \tag{35}$$

All other equations remain valid if n is replaced by n', in particular Eqs. (25)–(27), and contain even multiples of n.

2.4. Signal modulation

For a long mixing time, no detailed analytical results concerning the angular modulation have been reported by Mitra [3] which could be considered in the light of multiple concatenations. However, due to the larger exponent in Eqs. (8) and (31) it is expected that the signal modulation in the presence of microscopic anisotropy increases with n. This is investigated with numerical simulations (see below).

For a short mixing time, considering Eq. (27) reveals some of the interesting features of multiple concatenations. First, the signal decay $M_{\mathrm{iso}}(0,\theta) - M_{\mathrm{iso}}(q,\theta)$ for the antiparallel orientation ($\theta = \pi$) is given by $\frac{1}{3}\rho q^2\langle R^2\rangle$ and thus is independent of the number of concatenations n. This reflects the fact that for this orientation each intermediate rephasing gradient is immediately followed by a dephasing gradient of opposite polarity, i.e. the phase shifts introduced by these gradients are nulled for the short pulse durations assumed. Only the very first and the very last gradient of the gradient pulse series therefore yield effective phase shifts, and increasing the number of concatenations is equivalent to a prolongation of Δ. However, because $\Delta \gg \tau_D$ is assumed, the maximum dephasing effect a gradient pair may have is already supposed to be achieved for a single concatenation and an additional prolongation has no effect on the signal decay.

In contrast, the signal decay for parallel wave vector orientations ($\theta = 0$) according to Eq. (27) is given by $\frac{1}{3}\rho q^2\langle R^2\rangle(4n-1)$ which increases linearly with n. Taking the ratio of the signal decays expected for parallel and antiparallel wave vector orientations consequently yields

$$\frac{M_{\mathrm{iso}}(0,0) - M_{\mathrm{iso}}(q,0)}{M_{\mathrm{iso}}(0,\pi) - M_{\mathrm{iso}}(q,\pi)} = 4n - 1. \tag{36}$$

While for $n = 1$, i.e. the unconcatenated experiment, the signal decay for the parallel orientation of both wave vectors is three times of that for the antiparallel orientation, the ratio increases already to 7, i.e. is more than doubled, for two concatenations.

It should be emphasized that this increase represents a more pronounced signal modulation and not only an overall increased signal decay in the presence of multiple diffusion-weightings. This can be seen when comparing the modulation amplitude,

$$\frac{M_{\mathrm{iso}}(q,\pi) - M_{\mathrm{iso}}(q,0)}{2} = \frac{1}{3}\rho q^2\langle R^2\rangle(2n-1), \tag{37}$$

and the averaged signal decay which e.g. is obtained for a perpendicular wave vector orientation ($\theta = \pi/2$) and is

$$M_{\mathrm{iso}}\left(0,\frac{\pi}{2}\right) - M_{\mathrm{iso}}\left(q,\frac{\pi}{2}\right) = \frac{1}{3}\rho q^2\langle R^2\rangle 2n \tag{38}$$

Their ratio is given by

$$\frac{M_{\mathrm{iso}}(q,\pi) - M_{\mathrm{iso}}(q,0)}{2\left[M_{\mathrm{iso}}(0,\frac{\pi}{2}) - M_{\mathrm{iso}}(q,\frac{\pi}{2})\right]} = \frac{2n-1}{2n} = 1 - \frac{1}{2n} \tag{39}$$

which is $\frac{1}{2}$ for the unconcatenated experiment ($n = 1$) and asymptotically approaches 1 for a large number of concatenations n. This means that the relative signal modulation increases with n. Thus, it may be easier to detect, in particular in case that achieving a sufficient signal decay is difficult as on whole-body MR systems with their limited gradient amplitudes.

3. Experimental

To simulate the MR signal of diffusing spins in DWV experiments and analyze it with respect to the predicted signal behavior for short mixing times, a self-written IDL algorithm (version 6.4, ITT Visual Information Solutions, Boulder, Colorado, USA) was used. Its basic principles have been described previously [14], however, it was extended to handle multiple concatenations and used the generalized signal equations provided in the Theory section, i.e. Eqs. (23)–(27), for the fit procedures.

Prolate spheroidal pores with impermeable boundaries and semi-principal axes of 1.000 μm, 1.000 μm, and 3.163 μm, which effectively yields the same $\langle R^2 \rangle$ as the pores used in [14], were investigated. Relaxation effects were ignored. Five thousand spins were investigated with a temporal resolution of 10 μs and assuming a diffusion coefficient of 2.0×10^{-3} mm^2 s^{-1}. The gradient pulse duration was 10 μs to fulfill the short-pulse approximation. The diffusion time Δ was 30 ms, the mixing time τ_m either 10 μs or 30 ms to investigate the short and long mixing time regime, respectively. A minimum mixing time of δ was used to avoid an angular dependency of the diffusion-weighting b value which occurs for $\tau_m < \delta$ and introduces an additional signal modulation, even for free diffusing spins, that may interfere with the effect under investigation. Because τ_D (see above) can be estimated to be between 0.25 ms and 2.5 ms for the pores and the chosen diffusion coefficient (2.0×10^{-3} mm^2 s^{-1}), these values are in good agreement with the assumptions underlying the theoretical derivations ($\tau_m \ll \tau_D$ and $\tau_m \gg \tau_D$, respectively, and $\Delta \gg \tau_D$). One to five concatenations (n) were considered, for an half-integral number of concatenations n' values of $\frac{3}{2}$ and $\frac{5}{2}$ were used.

In all simulations, an identical magnitude of the two wave vectors was assumed ($q_1 = q_2 = q$). For the simulations with the short mixing time, the "isotropic", "tensor", and "trace" (x,y,z) direction schemes were used for the wave vector orientations [14]. They were designed either to investigate an isotropic orientation-distribution of the pores or to calculate the elements of the tensor $\mathbf{T}_n$ and derive the pore size measure $\langle R^2 \rangle$ and have been described in detail in [14]. In the isotropic scheme, 1651 directions were used for the first wave vector, for the second the same directions plus their inverted counterparts (3302 directions). This approach was chosen to ensure a sufficiently dense distribution of directions where parallel as well as antiparallel wave vector orientations are investigated.

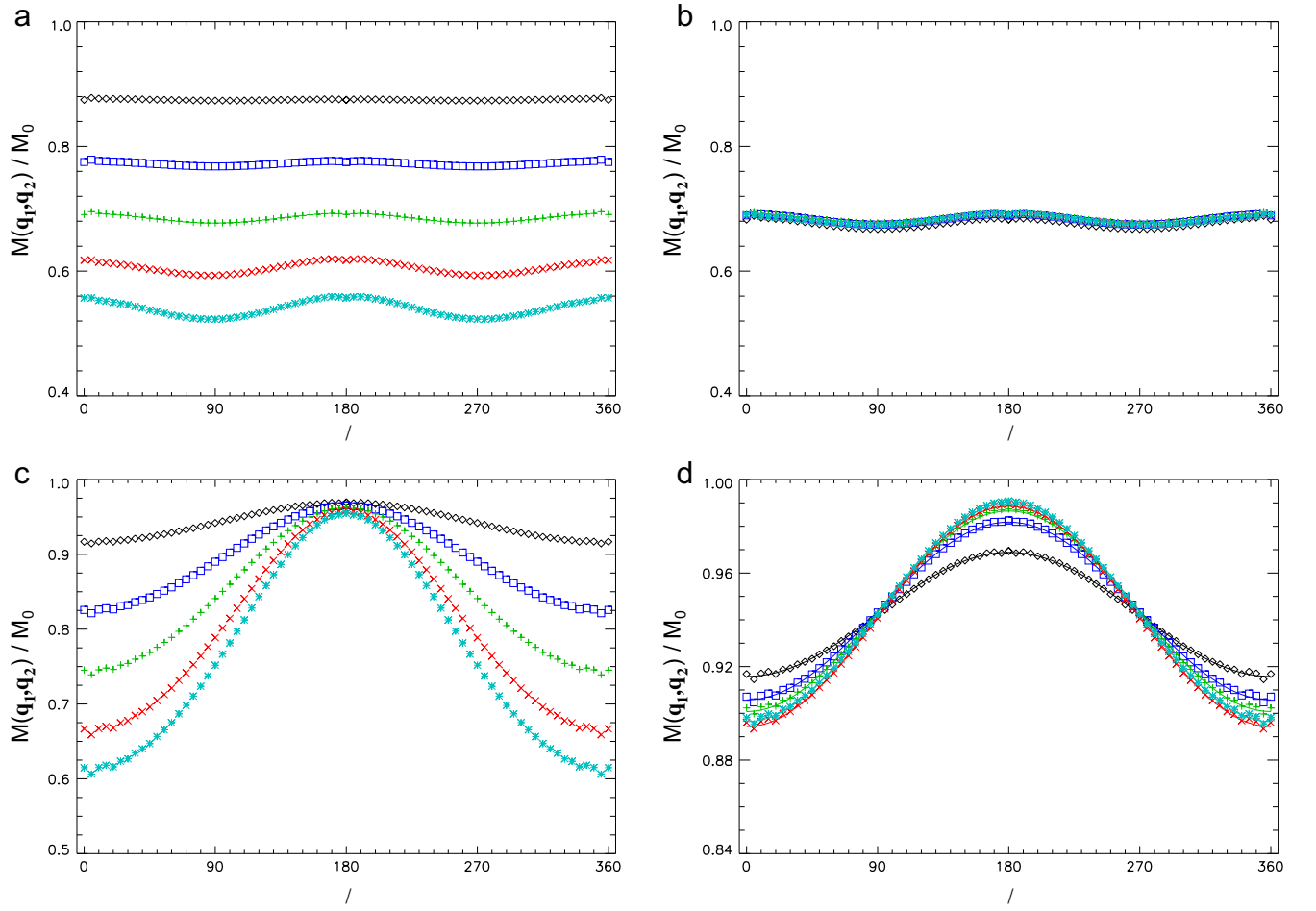

Fig. 2. Simulated MR signals (symbols) vs. the angle θ between the two wave vectors for an isotropic orientation-distribution of the ellipsoidal cells and one to five concatenations (diamond, square, +, ×, ∗) with (a,b) the long and (c,d) the short mixing time for (a,c) fixed gradient integrals q and (b,d) comparable signal decays. Simulations were performed for 5000 spins in ellipsoidal pores (semi-principal axis of 1.0 μm, 1.0 μm, and 3.2 μm) for a diffusion time Δ of 30 ms, a gradient pulse duration δ of 10 μs, and mixing times of 10 μs and 30 ms, respectively. To obtain a comparable signal decay as in (d), the product of the number of concatenations and q^2 was constant (about 0.9661 m^{-2}). The solid lines in (d) represent the fits to the theoretical curve, for details see text.

For the long mixing time, a modified isotropic scheme was used. Because the signal modulation is expected to yield a maximum difference between experiments with parallel and perpendicular wave vector orientations, a dense sampling of antiparallel orientations is not required. Instead, the total number of directions for the first wave vector was increased to 6599 and the same scheme was applied to both wave vectors in order to yield an increased sampling density of perpendicular wave vector orientations.

The simulations were analyzed as described previously [14]. The isotropic schemes were used to investigate both, the mean signal for an isotropic distribution of the pores and, for a short mixing time, the dependency of the signal on the wave vector orientations for a large range of orientations which also can be used to determine the elements of $\underline{\underline{\mathbf{T}}}_n$ and $\underline{\underline{\mathbf{R}}}$ for the full and the reduced tensor approach, respectively. As in [14], fits were based on a Levenberg–Marquardt algorithm.

4. Results

Fig. 2 shows the simulation results obtained for multiple concatenations and an isotropic orientation-distribution of the ellipsoidal cells. For a fixed gradient integral q, the averaged signal decay raises monotonically when increasing the number of concatenations (Fig. 2a and c) which reflects the increased diffusion weighting. For the short mixing time (Fig. 2c), the signal for the antiparallel orientation is not perfectly independent of the number of concatenations as expected. The slight decay observed with n can be assigned to the non-zero mixing time (10 μs). Although it is very short, it disturbs the complete nulling of the phase shifts of the two successive gradients. Doubling the mixing time increases the signal decay for the antiparallel orientations (data not shown) which demonstrates the influence of a small, but non-zero mixing time.

The increase with the number of concatenations also holds for the modulation amplitude (Fig. 2a and c). However, because an increased signal decay can also be achieved with a higher gradient pulse amplitude or a prolonged gradient pulse duration, a comparison for similar signal decays is more meaningful and shown in Fig. 2b and d. For the long mixing time, the modulation amplitude seems to be independent from the number of concatenations for a comparable signal decay (Fig. 2b). In contrast, it increases with the number concatenations for the short mixing time (Fig. 2d) as expected.

Some minor modulations are observed in the simulated data, e.g. at angles of 5°, due to a slightly anisotropic distribution of the wave vectors that enclose the corresponding angles. Increasing the number of directions is expected to reduce this effect. However, the calculation time for a single curve is already quite long with the more than 5.4 million (1651×3302) wave vector combinations currently used (33 h).

The fits to Eq. (27) shown in Fig. 2d (solid lines) are in good agreement with the simulations and yield a pore size which is within ±1.5% for the different numbers of concatenations. Compared to the nominal value, a slight underestimation of about 5% is present which similarly has been observed in previous studies [14]. It is consistent with higher (4th) order contributions in the simulations that are not taken into account in the theoretical considerations. Nevertheless, Eq. (27) seems to represent a good approximation of the signal modulation observed for pores with isotropic orientation-distribution.

In Fig. 3, the signal modulation observed in a sample with a single pore orientation is shown for some combinations of the isotropic direction scheme (Fig. 3a) and the full tensor scheme (Fig. 3b) for one to five concatenations. The signal range covered is extended compared to Fig. 2 because no averaging over isotropic pore orientations was performed, i.e. the data represent the signal observed in a sample with a single pore orientation. As in Fig. 2, the main effect of multiple concatenations is an increased modulation amplitude but there are also some changes in the shape of the curves, in particular for the isotropic scheme.

For both direction schemes, the fits to the tensor approach, i.e. to Eqs. (23) and (24), are in good agreement with the simulated

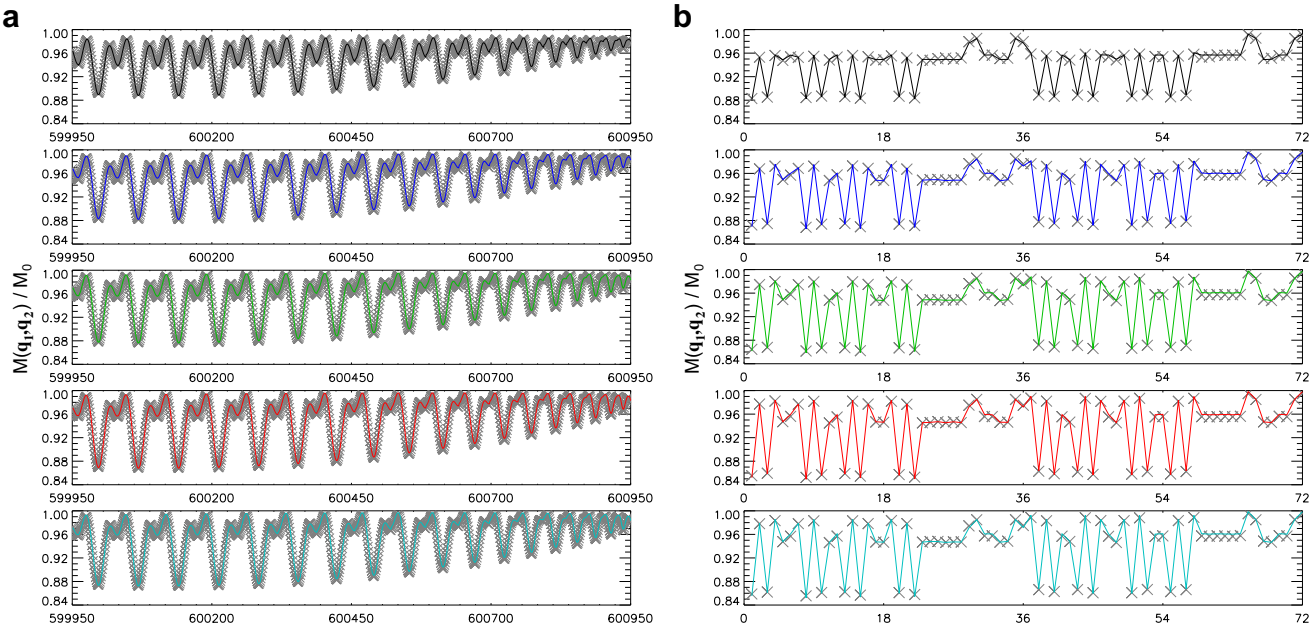

Fig. 3. Simulated MR signals (symbols) and corresponding fits (lines) to the extended tensor model for the short mixing time, pores of a single orientation, and one to five concatenations (upper to lower) with (a) the "isotropic" scheme and (b) the "tensor" scheme for the orientations of the wave vectors. The values of the abscissas represent the indexes of the wave vector orientation combinations plotted. In (a), only a minor part of the 5.5 millions different combinations (1651 orientations for the first, 3302 for the second wave vector) is shown but the fits were performed to all combinations. The product of the number of concatenations and q^2 was constant and about 0.9661 m^{-2}. For details see Fig. 2 and text.

data for all concatenations. The pore size parameters derived from the fits differ by less than 2% between the two direction schemes and are within ±5% of the nominal values with a slight underestimation for the long pore diameter and a minor overestimation for the shorter pore axis. Thus, the tensor approach extended for multiple concatenations can be considered to be a good model for the simulated data.

The simulations performed for parallel and antiparallel wave vector orientations in a sample with a single pore orientation are shown in Fig. 4 for the three direction schemes investigated and a comparable signal decay. Increasing the number of concatenations reduces the signal decay and modulation amplitude for the antiparallel orientation while they are increased for the parallel orientations (Fig. 4a). Accordingly, the signal difference of parallel and antiparallel orientations increases with the number of concatenations (Fig. 4b–d). The fits (solid lines) of the reduced tensor model adapted to multiple concatenations, i.e. according to Eq. (26), are in good agreement with the data simulated for the isotropic direction scheme (Fig. 4b) which validates the theoretical considerations.

The mean signal difference (dashed lines) over all orientations of the individual schemes yields very similar values for the different direction schemes and increases with the number of concatenations (Fig. 4b–d). It should be kept in mind that the gradient integral in these simulations was chosen to yield comparable signal decays for the different concatenation, i.e. $n \times q^2$ was constant. The signal modulation therefore does not increase with $2n-1$ as in Eq. (26) but is expected to be proportional to $1-\frac{1}{2n}$ as in Eq. (39). The ratio of the mean values obtained for the isotropic scheme and one and five concatenation is 0.5685 which is rather close to the theoretical value of $(1-\frac{1}{2\times1})/(1-\frac{1}{2\times5})=\frac{5}{9}$. Estimates of the pore radii derived from the isotropic scheme are within ±2% for the different concatenations with a slight, but systematic underestimation of about 5% compared to the nominal values. As pointed out earlier, this deviation is most likely due to higher order signal contributions. Mean pore size estimates obtained for the tensor scheme differ by about 1% from those of the isotropic scheme, those of the trace scheme by up to 4%. The larger deviation for the trace scheme could be related to the reduced number of directions which makes it more sensitive to numerical fluctuations.

In Fig. 5, the corresponding results for the half-integral numbers of concatenations ($\frac{3}{2}$ and $\frac{5}{2}$) are summarized. The mean curves for the isotropic orientation-distribution of the pores fit well between those for the larger and smaller integer numbers (one, two, and three concatenations, respectively) both for a constant gradient integral (Fig. 5a) and comparable signal decays (Fig. 5b). For a sample with a single pore orientation the fits of the corresponding tensor approach, i.e. using Eq. (35), are in a good agreement with the simulated data, both for the isotropic (Fig. 5c) and the tensor direction scheme (Fig. 5d). This also holds for the fits to Eq. (26) with $n=n'$, i.e. the reduced tensor model for the signal difference of parallel and antiparallel orientations (Fig. 5e).

The mean difference values (dashed lines) for the three direction schemes investigated for a single pore orientation (Fig. 5e–g) are very similar. The size estimates derived from these mean values are almost identical to the values for integer numbers of

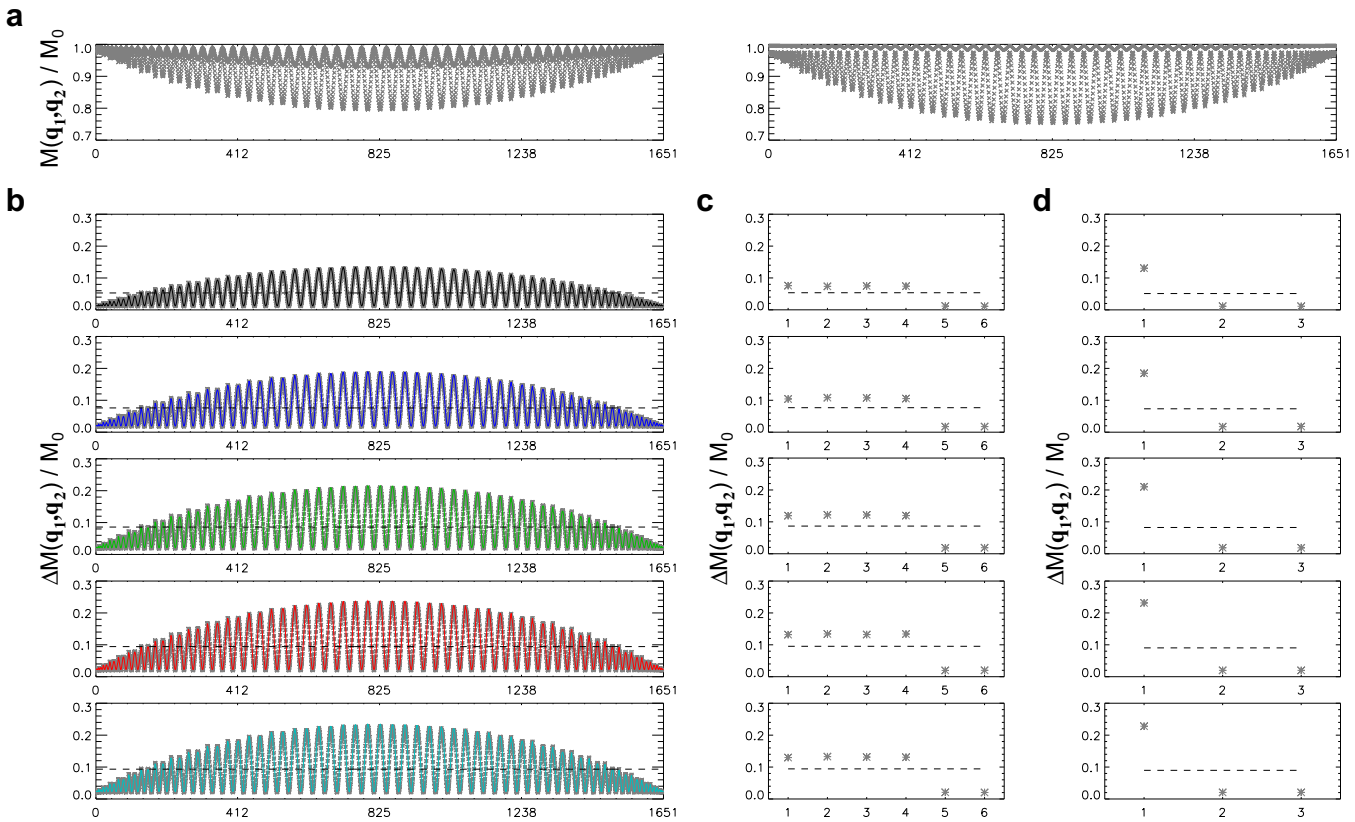

Fig. 4. (a) Simulated MR signals for one pore orientation and different wave vector orientations with parallel (upper,+) and antiparallel (lower,×) alignment of the two wave vectors for one (left) and five concatenations (right). (b–d) Signal differences (∗) for different wave vector orientations with parallel and antiparallel alignment of the two wave vectors and means of the signal differences (dashed lines) for the (b) isotropic, (c) tensor, and (d) "trace" direction schemes with one to five concatenations (upper to lower). The values of the abscissas represent the indexes of the wave vector orientation combinations plotted. The product of the number of concatenations and q^2 was constant to obtain a comparable signal decay (see Fig. 2d) and was about 0.9661 m^{-2}. The solid lines in (b) are the fits to the reduced tensor model adapted to multiple concatenations. All simulations were performed with the short mixing time, for details see Fig. 2 and text.

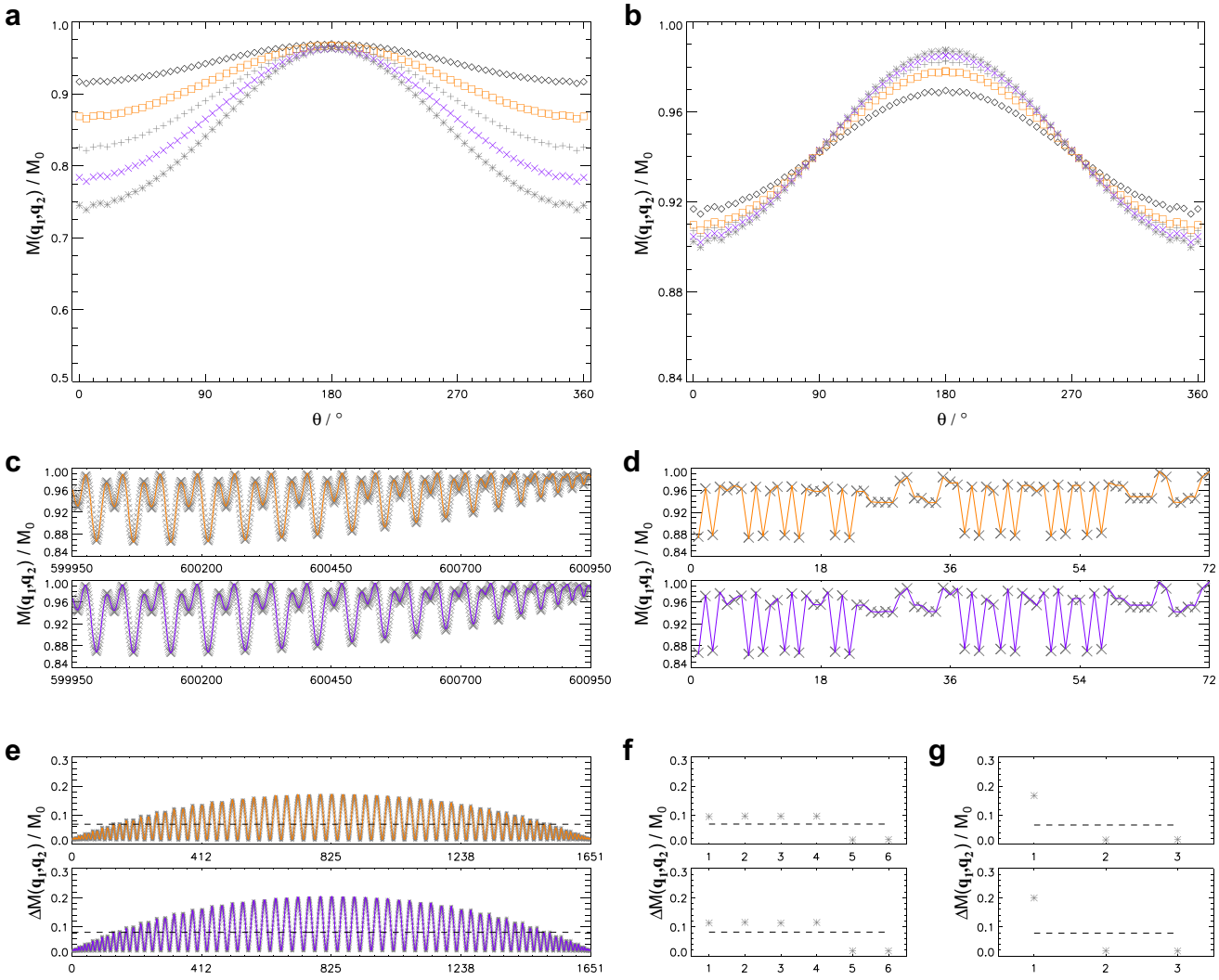

Fig. 5. Summarized simulation results for a half-integral number of concatenations, $\frac{3}{2}$ (squares/upper) and $\frac{5}{2}$ (×/lower), at the short mixing time. (a,b) Signal modulation with the angle between the two wave vectors for an isotropic orientation distribution of the ellipsoidal cells with (a) a fixed gradient amplitude and (b) a similar signal decay (constant $n \times q^2$). For comparison, the corresponding curves for integral numbers of concatenations (one, two, and three) are shown (diamond, +, ∗). (c,d) Signal modulation for a single pore orientation observed for (c) a subset of the isotropic direction scheme and (d) the tensor scheme. (e–g) Signal differences of parallel and antiparallel wave vector orientations for (e) the isotropic, (f) the tensor, and (g) the trace scheme. The values of the abscissas in (c–g) are the indexes of the wave vector orientation combinations plotted. The product of the number of concatenations and q^2 in (b–f) was about 0.9661 m^{-2}, i.e. identical to that used in Figs. 3 and 4. Symbols represent simulated signals, solid lines fits, dashed lines mean values over all orientations of the corresponding scheme. For details see Fig. 2 and text.

concatenations including the slightly overall reduction compared to the nominal values and the reduced values for the trace scheme. Thus, the presented theoretical approach for a half-integral number of concatenations is in a good agreement with the simulated data and behaves very analog to that for an integer number of concatenations.

5. Discussion

In this work, an extension of the standard DWV experiment is proposed which involves multiple concatenations of the two wave vectors. Although it has similarities to an experiment with multiple, i.e. more than two, wave vectors, the full flexibility that such an experiment can offer is not exploited here. Instead, the experiment is characterized by single values of the diffusion time, mixing time, and gradient pulse duration, the two wave vectors and the number of concatenations which is the only addition compared to a standard DWV experiment. Simplified expressions for the MR signal in case of a very long and a vanishing mixing time can be derived from the theoretical work of Mitra. For a vanishing mixing time, the expression reveals an increased amplitude of the signal modulation that is present when varying the angle between the two wave vectors, relative to the signal decay for a larger number of concatenations. Thus, the detectability of the signal modulation in experiments could be improved. The tensor approaches presented recently for vanishing mixing times have been extended to multiple concatenations and verified by numerical simulations.

In particular, experiments on whole-body MR systems could benefit from multiple concatenations. Because the gradient amplitudes available are very limited, long gradient pulses are required to achieve a signal decay sufficient to observe the signal modulation reliably. However, it has been shown for short mixing times that the modulation amplitude decreases for finite pulse durations [9,10,15,16], in particular if the pulse durations are in the order of τ_D or larger which is a realistic scenario for whole-body MR systems [11,12]. Multiple concatenations can ameliorate this problem because (i) the signal modulation for a comparable signal decay is

increased for a fixed pulse duration and (ii) the pulse duration can be reduced to achieve a comparable signal decay which further increases the modulation amplitude. The latter gain is expected to be in the order of the effect by the concatenations itself [9,10].

It should be noted that an increase of the signal modulation for shorter gradient pulses could also be expected for long mixing times. Thus, although the signal expressions derived for this experiment do not reveal a specific advantage for ideal conditions, it may benefit from multiple concatenations for realistic experiments, again in particular on whole-body MR systems.

In practice, the additional time required for multiple concatenations needs to be considered when optimizing the experiment since relaxation-related signal losses cannot be avoided. However, for experiments with short mixing times on whole-body MR systems the gradient pulse duration δ dominates the timing of the diffusion weighting [11]. Because δ typically is much larger than τ_D, it also causes an excessive diffusion time $\Delta \geqslant \delta$. With multiple concatenations, δ and the diffusion time as well can be shortened which can yield a reduced duration per diffusion-weighting. Because the amplitude of the signal modulation for a large number of concatenations asymptotically approaches double of the value present in a standard experiment, most of the gain achievable with multiple concatenations for a fixed gradient pulse duration is already obtained within the first few concatenations, e.g. 33% for 1.5, 50% for two, 75% for four concatenations. From this point-of-view, it could be expected that more than five concatenations are unattractive (less than 5% gain per additional concatenation). The additional gain of the signal modulation amplitude achieved with shorter δ is also needed for an optimization of the parameters but is quite difficult to calculate theoretically and may only be assessable with numerical simulations.

6. Conclusions

Multiple concatenations of two diffusion-weightings in a single experiment have been investigated as an extension of the standard double-wave-vector experiment and a special case of the more general multiple wave vector experiment. The signal expressions derived reveal an increased signal modulation amplitude for experiments with short mixing times which may help to improve the observability of the effect and to increase the accuracy of the experiments. An additional increase of the signal modulation can be expected due to the shorter gradient pulses usable with multiple concatenations which in particular is beneficial for experiments on whole-body MR systems with their limited gradient amplitude.

Acknowledgment

Parts of this work were supported by Bundesministerium für Bildung und Forschung (Neuroimage Nord).

Appendix A. Supplementary data

Supplementary data associated with this article can be found, in the online version, at doi:10.1016/j.jmr.2009.02.003.

References

[1] D.G. Cory, A.N. Garroway, J.B. Miller, Applications of spin transport as a probe of local geometry, Polym. Preprints 31 (1990) 149–150.
[2] P.T. Callaghan, B. Manz, Velocity exchange spectroscopy, J. Magn. Reson. A 106 (1994) 260–265.
[3] P.P. Mitra, Multiple wave-vector extensions of the NMR pulsed-field-gradient spin-echo diffusion measurement, Phys. Rev. B 51 (1995) 15074–15078.
[4] P.T. Callaghan, I. Furó, Diffusion–diffusion correlation and exchange as a signature for local order and dynamics, J. Chem. Phys. 120 (2004) 4032–4038.
[5] P.T. Callaghan, D. MacGowan, K.J. Packer, F.O. Zelayam, High-resolution q-space imaging in porous structures, J. Magn. Reson. 90 (1990) 177–182.
[6] Y. Cheng, D.G. Cory, Multiple scattering by NMR, J. Am. Chem. Soc. 121 (1999) 7935–7936.
[7] M.E. Komlosh, F. Horkay, R.Z. Freidlin, U. Nevo, Y. Assaf, P.J. Basser, Detection of microscopic anisotropy in gray matter and in a novel tissue phantom using double pulsed gradient spin echo MR, J. Magn. Reson. 189 (2007) 38–45.
[8] M.E. Komlosh, M.J. Lizak, F. Horkay, R.Z. Freidlin, P.J. Basser, Observation of microscopic diffusion anisotropy in the spinal cord using double-pulsed gradient spin echo MRI, Magn. Reson. Med. 59 (2008) 803–809.
[9] M.A. Koch, J. Finsterbusch, Numerical simulations of double wave vector diffusion experiments, in: Proceedings Int. Soc. Magn. Reson. Med., 14th Annual Meeting, Seattle, USA, 2006, p. 1631.
[10] M.A. Koch, J. Finsterbusch, Numerical simulations of double wave vector experiments investigating diffusion in randomly oriented ellipsoidal pores, Magn. Reson. Med. (2009), doi:10.1002/mrm.21976.
[11] M.A. Koch, J. Finsterbusch, Compartment size estimation with double wave vector diffusion-weighted imaging, Magn. Reson. Med. 60 (2008) 90–101.
[12] M.A. Koch, J. Finsterbusch, Double wave vector diffusion weighting in the human corticospinal tract in vivo, in: Proceedings Int. Soc. Magn. Reson. Med., 14th Annual Meeting, Toronto, Canada, 2008, p. 764.
[13] E. Özarslan, P.J. Basser, Microscopic anisotropy revealed by NMR double pulsed field gradient experiments with arbitrary timing parameters, J. Chem. Phys. 128 (2008) 154511-1–154511-11.
[14] J. Finsterbusch, M.A. Koch, A tensor approach to double wave vector diffusion-weighting experiments on restricted diffusion, J. Magn. Reson. 195 (2008) 23–32.
[15] C.H. Ziener, T. Weber, W.R. Bauer, P.M. Jakob, Quantification of the spinal cord axon diameter using an extension of the PGSE sequence, in: Proceedings Int. Soc. Magn. Reson. Med., 15th Annual Meeting, Berlin, Germany, 2007, p. 13.
[16] T. Weber, C.H. Ziener, T. Kampf, V. Herold, W.R. Bauer, P.M. Jakob, Measurement of apparent cell radii using a multiple wave vector diffusion experiment, Magn. Reson. Med. (2009), doi:10.1002/mrm.21848.